Title
ANTINEUTRON PRODUCTION BY CHARGE EXCHANGE

Authors
Button, Janice
Elioff, Tom
Segre, Emilio
et al.

Publication Date
1957-07-29

UCRL 3883

UNIVERSITY OF CALIFORNIA

Radiation Laboratory

BERKELEY, CALIFORNIA

UCRL-3883

UNIVERSITY OF CALIFORNIA

Radiation Laboratory
Berkeley, California

Contract No. W-7405-eng-48

ANTINEUTRON PRODUCTION BY CHARGE EXCHANGE

Janice Button, Tom Elioff, Emilio Segrè, Herbert M. Steiner,
Richard Weingart, Clyde Wiegand, Tom Ypsilantis

July 29, 1957

Printed for the U. S. Atomic Energy Commission

ANTINEUTRON PRODUCTION BY CHARGE EXCHANGE

Janice Button, Tom Elioff, Emilio Segrè, Herbert M. Steiner, Richard Weingart, Clyde Wiegand, Tom Ypsilantis

Radiation Laboratory
University of California
Berkeley, California

July 29, 1957

ABSTRACT

Antineutrons produced by 440-Mev antiprotons incident upon Pb, C and CH_2 targets have been observed. The antineutrons were detected by their energy release upon annihilation. Charge-exchange cross sections for antiprotons in the three targets have been calculated. The results show that the effective charge-exchange cross section per proton of the target nucleus decreases rapidly with increasing Z.

ANTINEUTRON PRODUCTION BY CHARGE EXCHANGE*

Janice Button, Tom Elioff, Emilio Segrè, Herbert M. Steiner, Richard Weingart, Clyde Wiegand, Tom Ypsilantis

Radiation Laboratory
University of California
Berkeley, California

July 29, 1957

I. Introduction

The observation of antiprotons produced in high-energy nucleon-nucleon collisions led us to believe that antineutrons are also created in such processes by charge exchange.[1] This process has been recently observed by Cork, Lambertson, Piccioni, and Wenzel.[2] The antineutron, like the neutron, is electrically neutral, but it has a magnetic moment that is parallel to its spin angular momentum, in contrast to the neutron, for which these two vectors are antiparallel. Because the antineutron has zero charge, a mass spectrograph similar to that employed in identifying the antiproton[3] could not be used to observe the antineutron.

Antineutrons are able to annihilate in ordinary matter with the subsequent release of 2 Bev of energy. We have utilized this property, which is characteristic of antinucleons, to detect the antineutron. For this purpose a counter was constructed in which the annihilation process could be detected. This counter was constructed to satisfy two requirements: first, a large fraction of the 2 Bev of energy released upon antinucleon annihilation must be spent within the counter without any appreciable fraction escaping through the sides; secondly, the response of the counter should be a monotonic function of the energy deposited in it. Antineutrons produced directly by nucleon-nucleon collisions are difficult to detect by this method because

---

*This work was performed under the auspices of the U. S. Atomic Energy Commission.

[1]Chamberlain, Segrè, Wiegand, and Ypsilantis - Nature 177, 11 (1956).

[2]Cork, Lambertson, Piccioni, and Wenzel, Phys. Rev. 104, 1193 (1956).

[3]Chamberlain, Segrè, Wiegand, and Ypsilantis, Phys. Rev. 100, 947 (1955).

of the presence of a background of very-high-energy neutrons that can deposit energies in the counter that are comparable to the annihilation energy. We therefore sought an alternative method for production of these particles. In analogy to the observed n-p charge-exchange scattering, it is reasonable to expect that antiprotons also are capable of undergoing an exchange process with protons of ordinary matter, thereby producing a neutron-antineutron pair.[1] We have utilized this method of production to observe antineutrons produced by 1080-Mev/c antiprotons incident on Pb, C, and CH_2 targets. Charge-exchange cross sections for these materials have been calculated from the experimental data on the assumption that the attenuation of antineutrons is identical to that of antiprotons.

II. Experimental Procedure

A well-defined beam of 1080-Mev/c negatively charged particles, containing antiprotons and lighter particles (mostly π mesons) in the ratio of 1:30, 000 was incident upon the antineutron production-detection system shown in Fig. 1. Approximately 10 antiprotons per minute entered this system through the 4-inch-diameter scintillation counter, S1. The antiprotons were identified by a system of analyzing magnets and counters described in the preceding article.[4]

The counter S1 was the last counter of the antiproton-identifying system. Counter C* was a Cerenkov counter filled with methyl alcohol and slotted as shown to accommodate various targets. It was the purpose of this counter to distinguish between inelastic events in the target involving the emission of charged particles with $\beta > 0.75$ and all other processes. The particles registering in this counter were predominately fast charged pions arising from annihilations in the target or in the methyl alcohol of the counter. Counter C* has been described in the preceding paper.[4] S4 and S5

---

[4] See preceding article, "Antiproton Interactions in Complex Nuclei."

were plastic scintillation counters that were used as "guard" counters to discriminate between charged and neutral particles entering Counter D. Counter D was used to distinguish between antinucleons and all other particles entering it, on the basis of their energy release in D. This counter was constructed in the form of a multilayer sandwich of lead and plastic scintillator viewed by 48 photomultiplier tubes. This type of construction enabled us to obtain a rather thorough sampling of the energy released by various particles in this counter.

Antiprotons arriving at the target could undergo annihilation, suffer elastic or inelastic scattering, pass through the target and Cerenkov counter C* without any nuclear interaction, or undergo a charge-exchange process resulting in the formation of a neutron-antineutron pair. Annihilations in the target were in most cases characterized by large pulses in the Cerenkov counter C*. Scattering, pass-through, and charge-exchange events either did not register in C* or were accompanied by only an occasional small pulse in this counter (the source of these small pulses is discussed in the preceding paper). The formation of an antineutron in the target should thus be characterized by the signal of the arrival of an antiproton in S1 followed by: no pulse in C*, no pulse in the subsequent scintillation counters S4 and S5, and a pulse in D of a size commensurate with that produced by an antinucleon annihilation in D (i.e., S1, $\overline{C*}$, $\overline{S4}$, $\overline{S5}$, large pulse in D). The pulse size corresponding to antinucleon annihilation in D was obtained by calibrating this counter with antiprotons.

The function of C* was to detect fast charged pions produced in the annihilation of an antiproton in the target, but there is a small probability that the fast pions produced in the annihilation are all neutral, in which case the Cerenkov counter C* may not register a pulse. The gamma rays resulting from these neutral pions could simulate antineutrons by giving rise to large pulses in D without being detected by the guard counters. It was the purpose of the 1.5 inches of lead between counters S4 and S5 to convert these gamma rays. In the first run with the CH_2 target, Counter C* was connected in anticoincidence with the others in such a way that an antineutron was defined by a signal from S1 indicating the incidence of an antiproton on the target followed by $\overline{C*}$, $\overline{S4}$, $\overline{S5}$, and a large pulse in D. We found that the information given by C* was redundant because whenever $\overline{S4}$, $\overline{S5}$ occurred in coincidence with a large pulse in D there was no pulse in C*. It was then decided to remove the Cerenkov counter C* for the subsequent runs on carbon and lead.

The pulses from all counters were displayed on a four-sweep oscilloscope and recorded photographically. The oscilloscope was triggered each time an antiproton passed through counter S1 into the system shown in Fig. 1. A record of the type of interaction for each antiproton entering the target was obtained in this way. Three different types of events are shown in Fig. 2 for the CH_2 target.

The primary purpose of Counter D was to contain the 2 Bev of energy given up upon antinucleon annihilation in this counter, thereby enabling one to differentiate between antinucleons and other particles passing into it. It was constructed of 48 identical cells measuring 24 by 12 by 2 in., each with a sensitive area of 12 by 12 in. Each cell contained a 12-by-12-by-2-in. lucite light pipe, six 12-by-12-by-0.25-in. plastic scintillators, and five 12-by-12-in. lead sheets 0.090 in. thick which were sandwiched between alternate layers of the plastic scintillator. The scintillators were cemented to the lucite with Epon (Shell Chemical Corp. product), and this entire unit was then enclosed in a light tight steel box. Each cell was viewed by a RCA 6810 photomultiplier tube. A typical cell is shown in Fig. 3. The 48 individual cells were assembled in layers, four cells per layer, so that the entire counter was 12 cells thick along the beam direction. A view of the assembled counter is shown in Fig. 4. The active volume of this counter formed a cube roughly 2 feet on a side whose average density was 3.84 g/cm^3. The assembled counter weighed 2.5 tons. The thickness along the beam direction was 156 g/cm^2 lead, 45.7 g/cm^2 plastic scintillator, and 60 g/cm^2 iron (from the steel covers of the individual cells). This counter presented approximately three annihilation mean free paths to incident antinucleons. The ionization energy loss of charged particles traversing D was divided in such a way that about 47% was spent in the lead, 25% in the iron, and 28% in the plastic scintillator.

Range-energy relations indicate that a 1080-Mev/c antiproton is capable of penetrating at most only 16-in. into this counter. Therefore all antiprotons incident upon the central region of D were expected to annihilate. The observed antiproton spectrum for 2000 events is shown in Fig. 5. Most of the "tail" of this curve at small pulse heights ($<$ 6 mm) is attributed to antiprotons that annihilated in the lead converter between counters S4 and S5. An additional contribution is due to antiprotons that were scattered by the target and converter into the outer region of D. The dashed histogram is the spectrum obtained from negative pions of the same momentum. In Fig. 6 the distribution of pulses produced in D by positive protons of 450 Mev has been plotted. Calibration of D on the basis of the positive-proton spectrum leads to an apparent average antiproton energy release of 1350 Mev in the D counter.

III. Experimental Results

Antineutrons that are produced by charge exchange and are projected forward so as to enter D must be characterized by $\overline{C^*}$ (when Counter C* is present), $\overline{S4}$, and $\overline{S5}$. All events satisfying this condition are recorded in Fig. 7 with the accompanying pulse height in D. In order to confirm the interpretation of these pulses as due to antineutrons we require also that there should be a pulse in D comparable to those observed from antiproton annihilations in this counter. The large pulses appear to be quite consistent with the antiproton spectrum. The grouping at small pulse heights is most probably caused by

(a) inelastic events in the target that have resulted in the entry of neutral particles other than antineutrons into D without giving rise to a pulse in C*;

(b) antiprotons that have annihilated in the insensitive portion of the D counter, a small part of which was not guarded by the scintillators S4 and S5;

(c) antineutrons produced at an angle with respect to the beam direction such that they were incident near the edge of the active volume of Counter D.

Events of the types (a) and (b) have been observed in other phases of our work to give rise to pulses as large as 5 mm in D. In view of this and also of the requirement that antineutron pulses in D be large, we have classified as antineutrons only those events giving pulses of 7 mm or more in Counter D. On the basis of the antiproton spectra in D we estimate that approximately 10% of the antineutrons entering this counter give rise to pulse less than 7 mm. One possible reason for these small pulses is Case (c) --if an antineutron enters near the edge of the active volume of D it may deposit only a small fraction of the annihilation energy in the counter, in which case it causes only a small pulse. In determining the effective solid angle subtended by D (at the target) we imposed the requirement that all antineutrons produced into this solid angle should have an opportunity to traverse at least one mean free path for annihilation before escaping from the counter. By assuming an annihilation mean free path in D for the antineutron equal to that for an antiproton we have determined this effective solid angle to be 0.275 steradian, corresponding to a cutoff angle of 17°. This angle is shown in Fig. 1.

In Table I we have summarized the results obtained for each of the targets. The charge-exchange cross sections were determined from the expression

$$\sigma_c = \frac{I(\bar{n})}{I(\bar{p})\, N_{tgt}} \exp\left(N_{tgt}\,\sigma_{tgt} + N_{sc}\sigma_{sc} + N_{Pb}\sigma_{Pb}\right),$$

where σ_c = charge-exchange cross section per molecule for production of antineutrons into a solid angle of 0.275 steradian in the forward direction,

$I(\bar{p})$ = total number of antiprotons incident on the target,

$I(\bar{n})$ = total number of antineutrons observed in D,

$\exp(N_{tgt}\sigma_{tgt})$, $\exp(N_{sc}\sigma_{sc})$, and $\exp(N_{Pb}\sigma_{Pb})$ are the attenuations in the target, the scintillation counters S4 and S5, and the 1.5-in. Pb converter, respectively. The product of these attenuation factors is between 3 and 4 for all targets if we assume the same attenuation cross sections for antineutrons of the energies in this experiment as for 450-Mev antiprotons.

The values for these cross sections are given in the preceding two papers.

Table I. Summary of experimental results. $I(\bar{p})$ is the total number of incident antiprotons, $I(\bar{n})$ is the observed number of antineutrons, and $\bar{T}_{\bar{p}}$ is the average antiproton energy in the target; σ_c is the charge-exchange cross section per molecule for production of an antineutron into a solid angle of 0.275 steradian in the forward direction.

Target	Thickness (g/cm^2)	$I(\bar{p})$	$I(\bar{n})$	σ_c (mb)	$\bar{T}_{\bar{p}}$ (MeV)
CH_2	21.4	3647	13	$10.0^{+2.8}_{-2.8}$	455
C	44.6	2738	6	$4.0^{+1.6}_{-1.5}$	434
Pb	86.4	3125	1	$3.8^{+4.2}_{-2.5}$	426

The CH_2 target was used together with the Cerenkov counter C*, which contained 11.07 g/cm^2 of methyl alcohol, CH_3OH. We have considered the oxygen atom in the alcohol molecule equivalent to a carbon atom, in the production of antineutrons. Because it appears that the charge-exchange cross section does not vary rapidly with Z, this step is justified. This assumption leads to the effective CH_2 target thickness given in Table I.

A value for $\sigma(\bar{p} + p \rightarrow \bar{n} + n)$ can be obtained from the CH_2 and C data by subtraction. We find

$$\sigma(\bar{p} + p \rightarrow \bar{n} + n) = (3.0 \pm 1.6) \times 10^{-27} \text{ cm}^2$$

for antineutron production by protons into a solid angle of 0.275 steradian in the forward direction. This value corresponds to a differential cross section of $(10.9 \pm 5.8) \times 10^{-27}$ cm^2/steradian averaged over a cone of half-angle 17° in the forward direction.

The charge-exchange cross section for carbon given above should be compared with the estimate of 8×10^{-27} cm^2 given by Cork, Lambertson, Piccioni, and Wenzel[3] for charge exchange into a comparable solid angle.

IV. Discussion

The experimental results show that the charge-exchange cross sections for lead, carbon, and hydrogen are the same within statistical limits. This indicates that the effective charge-exchange cross section per proton of the target nucleus decreases rapidly with increasing Z. Much of this effect can be attributed to the large nucleon-antinucleon annihilation cross section. In the first place this large cross section prevents antiprotons from penetrating into the nucleus, thus leaving only the hemispherical surface of the nucleus, which the beam strikes first, effective in producing antineutrons. Secondly, most of the antineutrons that are produced in the forward direction at this surface are swallowed up before they can escape from the nucleus. We may therefore expect that observable antineutrons are produced only when the incident antiprotons make a grazing collision with the nucleus. Neutron-antiproton collisions are less likely to give rise to antineutrons than proton-antiproton collisions because the emission of an antineutron in a $\overline{p}n$ collision requires the formation of at least one negative pion, which is energetically unfavorable and probably competes poorly with annihilation. These circumstances add two reasons for depressing charge exchange further in heavy nuclei: the ratio N/Z is higher in heavy nuclei than in light nuclei, and there is reason to believe that there are more neutrons than protons near the surface of these nuclei.[5, 6]

If we assume that the angular distribution of the $\overline{p}p$ charge-exchange cross section is the same as that for the n-p exchange process, we find that approximately 40% of the charge- exchange antineutrons were produced into the solid angle defined by Counter D. This comparison also leads to an estimate of the $\overline{p} + p \rightarrow \overline{n} + n$ differential cross section at 0° in the lab system of 38 ± 20 mb, which is to be compared with a value of 54 mb at the same lab angle for the p-n charge-exchange cross section at 400 Mev.[7]

---

[5] R. C. P. Voss and R. Wilson, Phys. Rev, 99, 1056 (1955).

[6] O. Miyatake and C. Goodman, Phys. Rev. 99, 1040 (1955).

[7] Hartzler, Siegel, and Opitz, Phys. Rev. 95, 591 (1954).

Charge independence requires that the following inequality be satisfied:

$$\frac{d\sigma(0^o)}{d\Omega}_{\bar{p}p \rightarrow \bar{n}n} \geqslant \left(\frac{k}{4\pi}\right)^2 \left[\sigma^{total}_{\bar{p}n} - \sigma^{total}_{\bar{p}p}\right]^2 ,$$

where k is the wave number of the incident antiproton in the laboratory system. If we assume the value for the charge-exchange cross section at 0^o stated above, then the difference between the total antiproton-proton and the antiproton-neutron cross sections at 440 Mev must be less than 50mb. The $\bar{p}$-p and $\bar{p}$-n cross sections quoted in the preceding paper are consistent with this prediction.

- - - - - - - - - - - - - -

We wish to thank Dr. Edward J. Lofgren and the staff at the Bevatron for their cooperation.

Figure Captions

Fig. 1. Experimental arrangement.

Fig. 2. Oscilloscope record of three antiproton events in the target. The pulses from counters identifying the antiproton are displayed on the top sweep. The signals from the Cerenkov counter C*; the scintillators S1, S4, and S5; and the counter D were displayed on the lower three sweeps as shown.

(a) An Antiproton annihilation in the target sending charged particles into D.

(b) An antiproton pass-through into D.

(c). An antineutron produced in the target and passing into D.

Fig. 3. A typical cell of Counter D. The steel cover and the end plate have been removed, exposing the laminations of lead and plastic scintillator as well as the lucite light pipe.

Fig. 4. The assembled Counter D.

Fig. 5. The histogram is the antiproton pulse-height distribution in the D counter for 2000 "pass-through" events in the CH_2 target. The smooth curve is the π^- spectrum obtained under the same conditions.

Fig. 6. Pulse-height distribution in D for 450-Mev positive protons incident on this counter.

Fig. 7 Pulse-height distribution in Counter D for all events that did not register in S4, S5 and the Cerenkov counter.

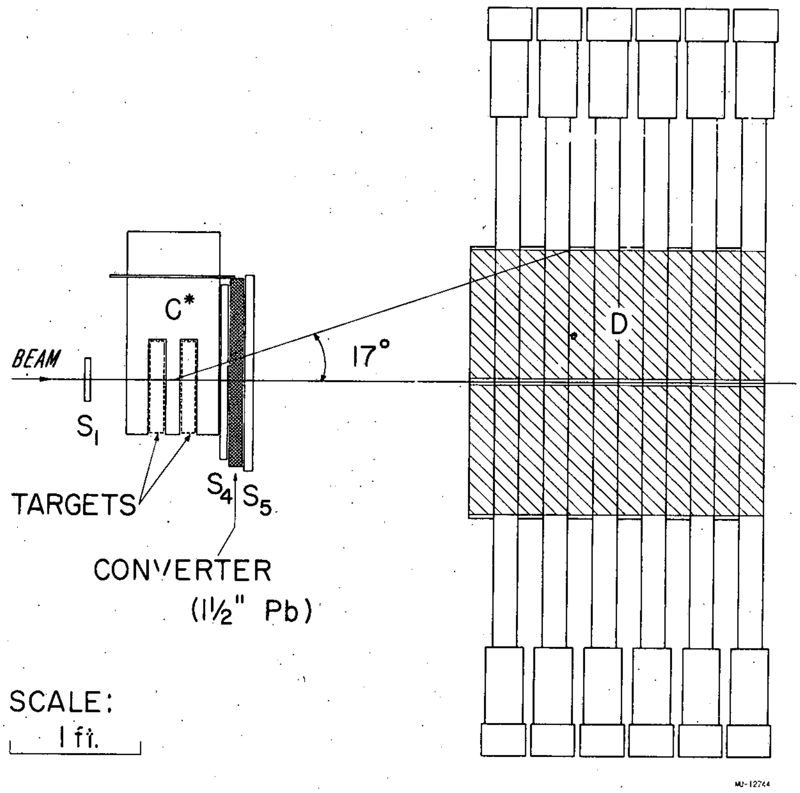

Fig. 1

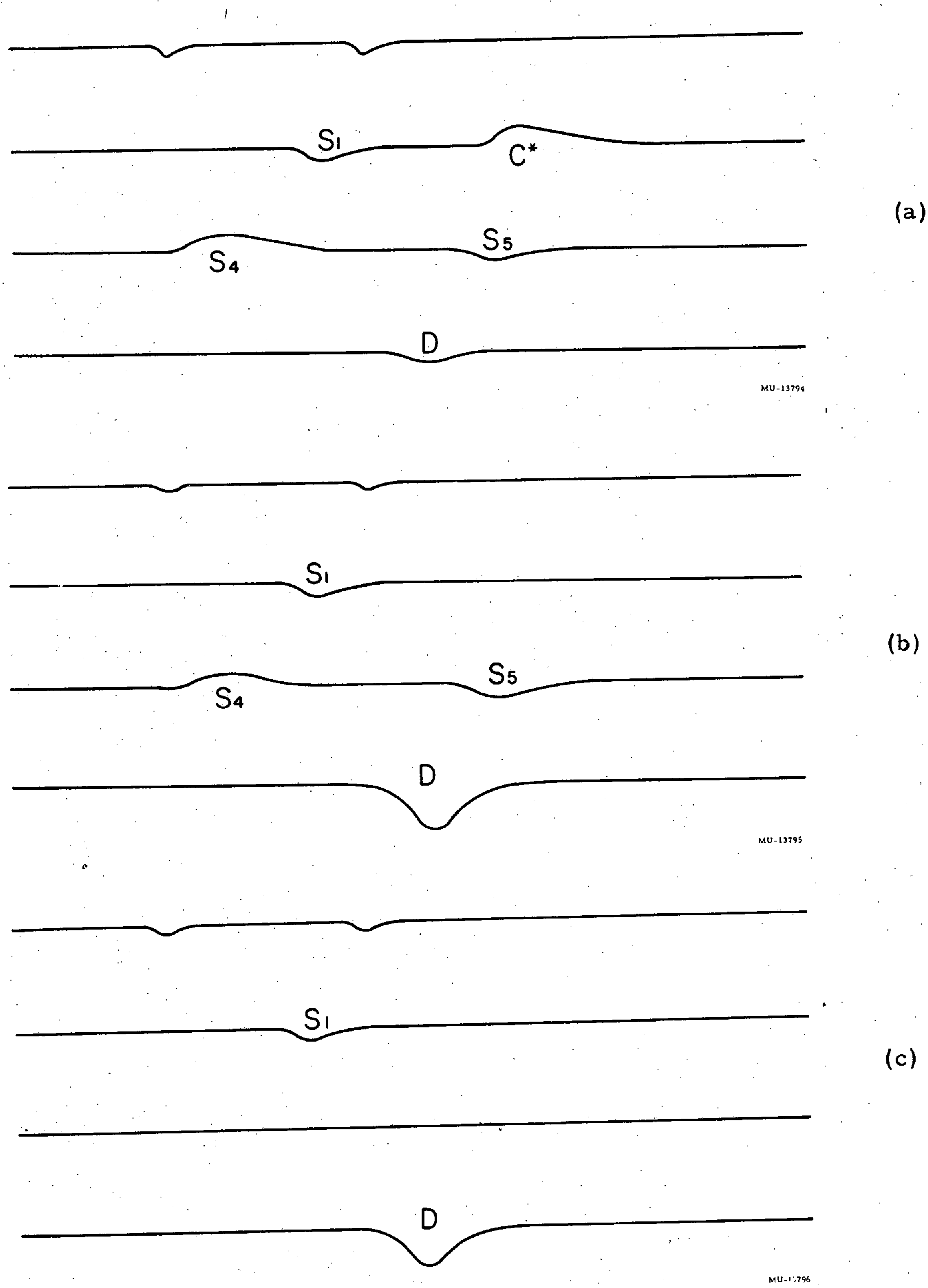

Fig. 2

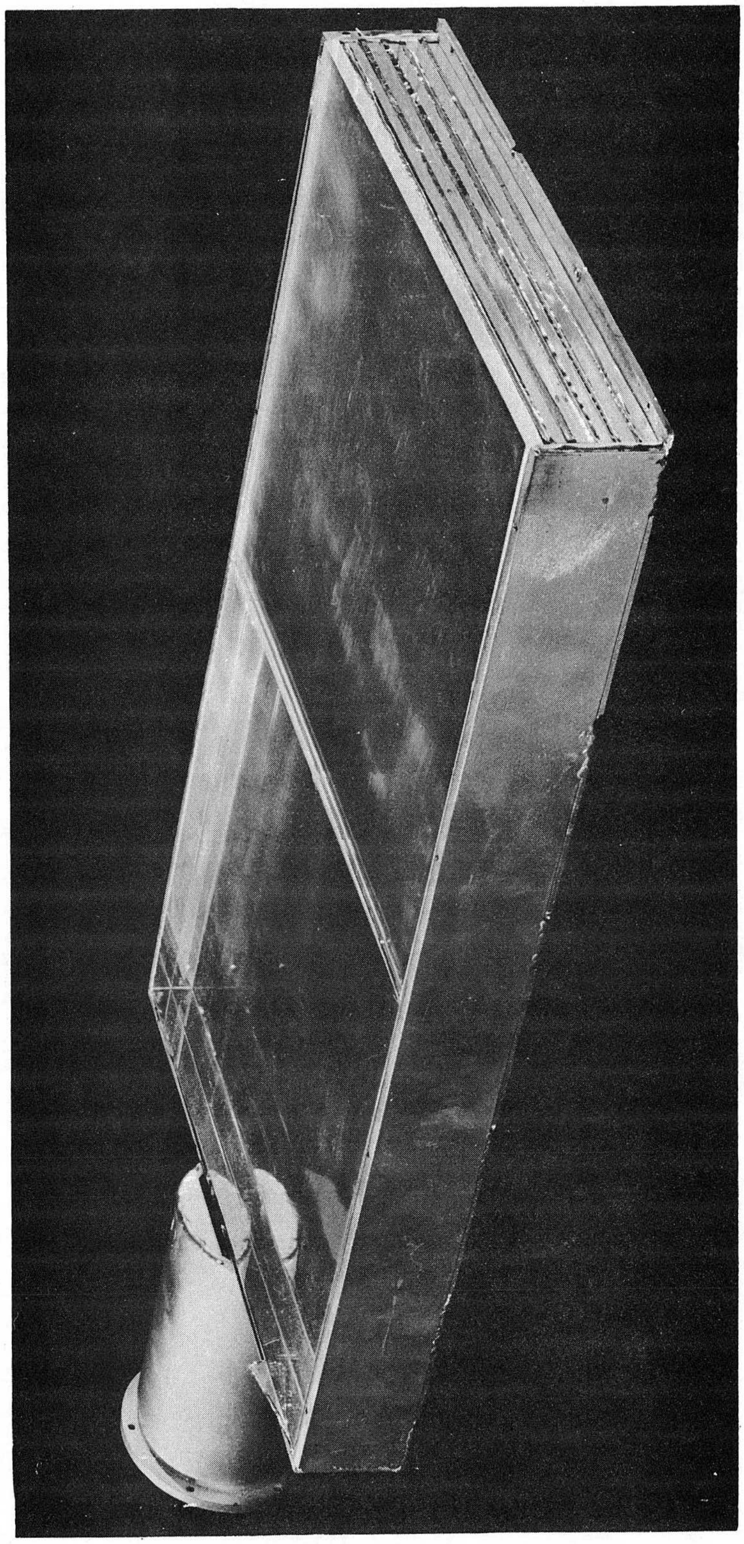

ZN-1604

Fig. 3

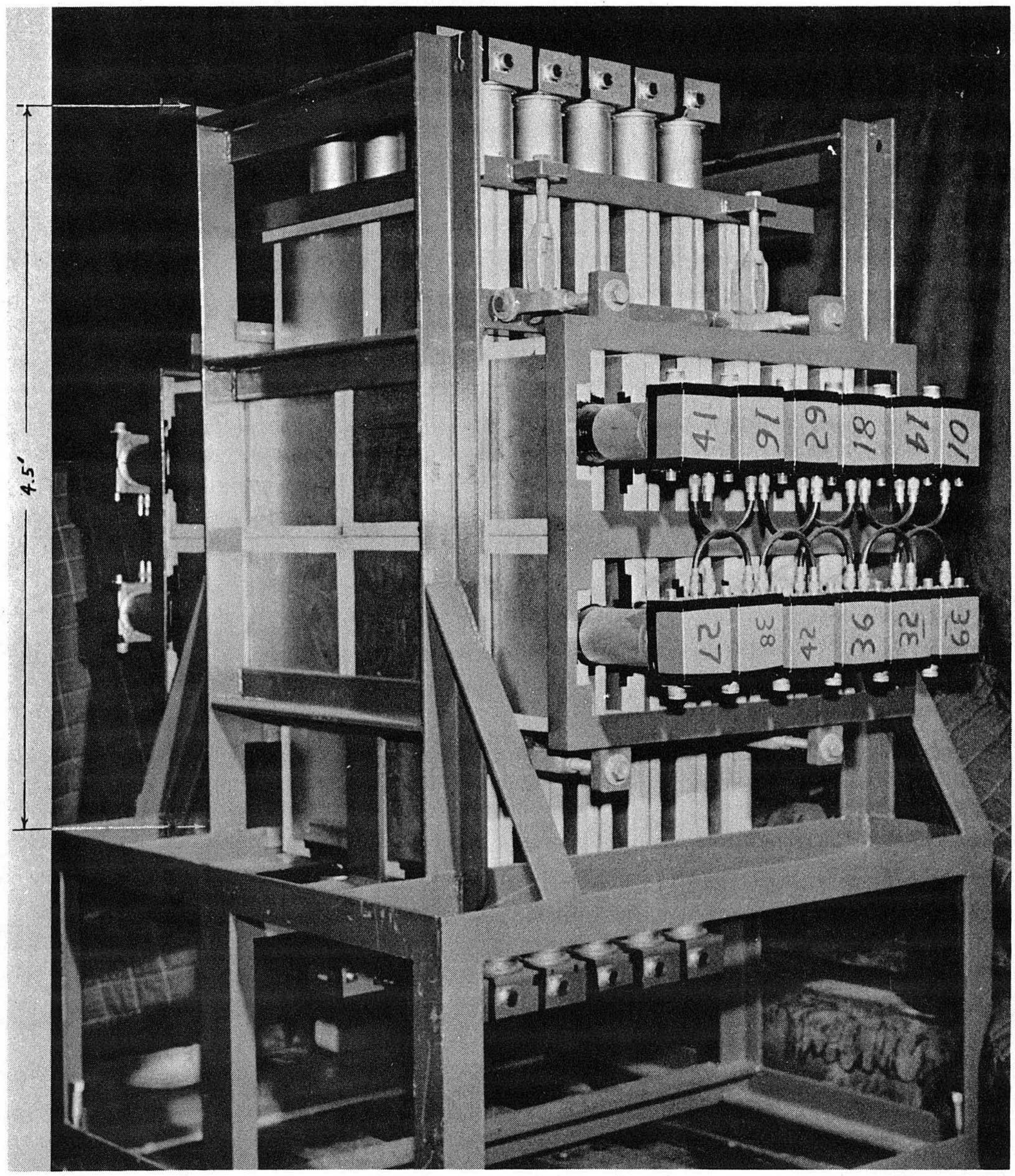

ZN-1747

Fig. 4

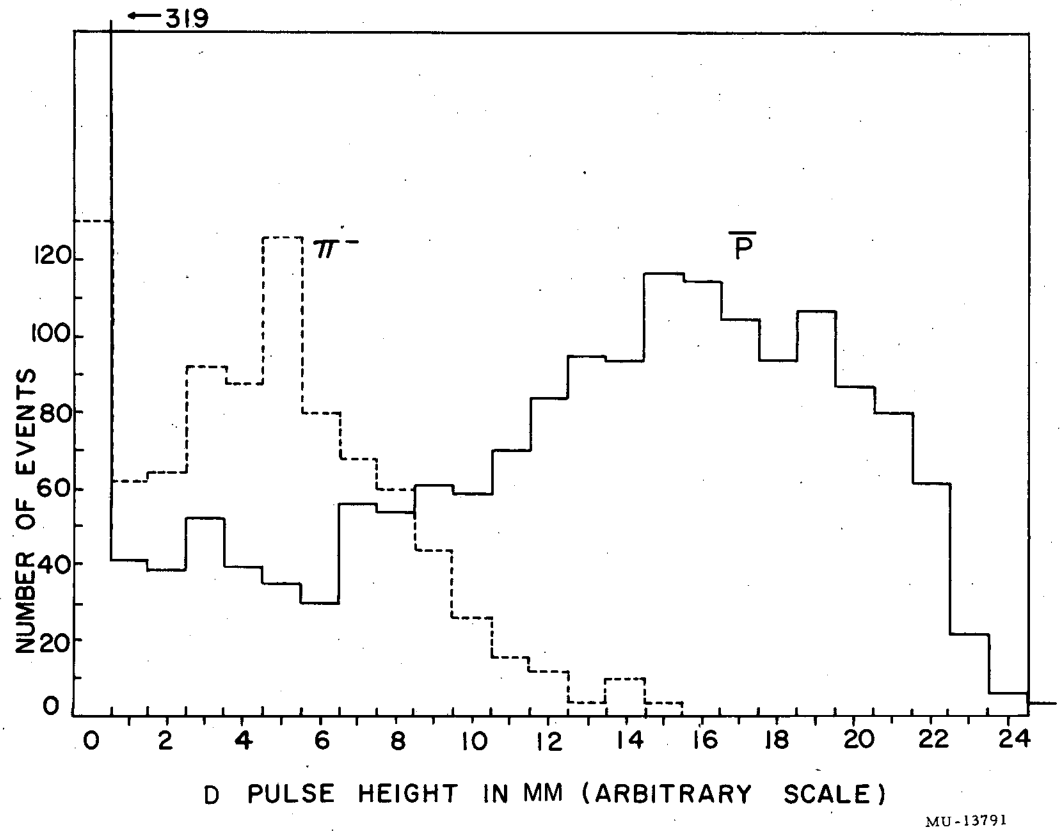
319
π^-
$\overline{P}$
NUMBER OF EVENTS
0
20
40
60
80
100
120
0 2 4 6 8 10 12 14 16 18 20 22 24
D PULSE HEIGHT IN MM (ARBITRARY SCALE)
MU-13791

Fig. 5

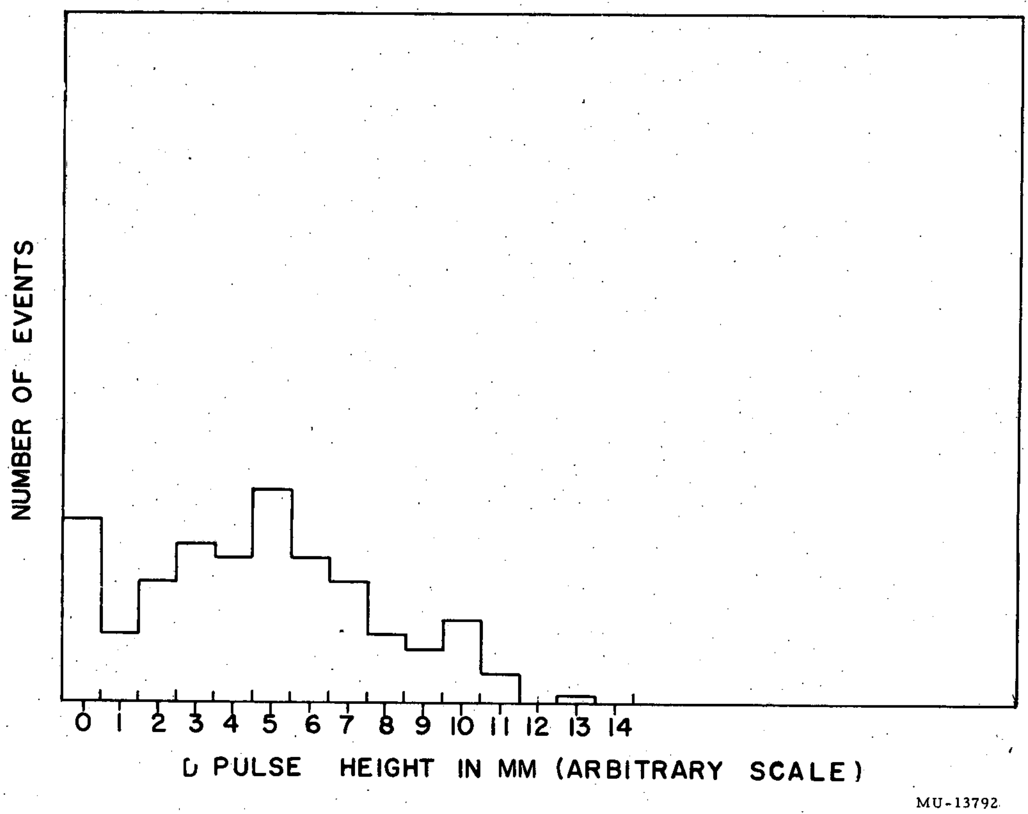
NUMBER OF EVENTS
0 1 2 3 4 5 6 7 8 9 10 11 12 13 14
D PULSE HEIGHT IN MM (ARBITRARY SCALE)
MU-13792

Fig. 6

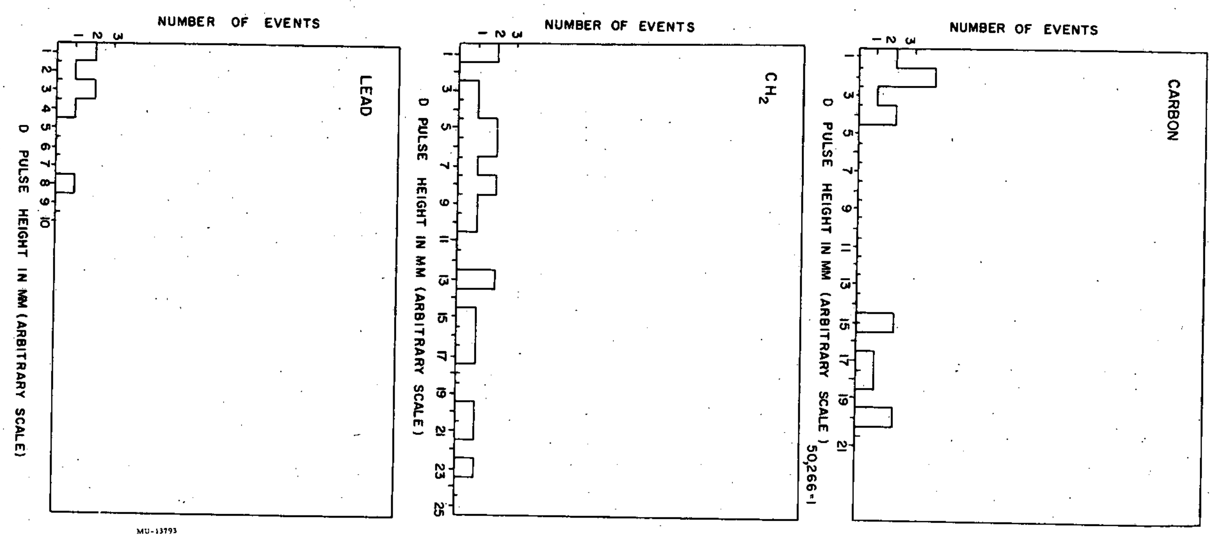
NUMBER OF EVENTS
LEAD
D PULSE HEIGHT IN MM (ARBITRARY SCALE)
CH2
CARBON
50,266-1
MU-13793

Fig. 7